

An accurate spectral method for solving the Schrödinger equation.

G. H. Rawitscher

Physics Department, University of Connecticut, Storrs, CT 06269-3046

I. Koltracht

Mathematics Department, University of Connecticut, Storrs, CT 06269-3009

Abstract

The solution of the Lippman-Schwinger (L-S) integral equation is equivalent to the the solution of the Schrödinger equation. A new numerical algorithm for solving the L-S equation is described in simple terms, and its high accuracy is confirmed for several physical situations. They are: the scattering of an electron from a static hydrogen atom in the presence of exchange, the scattering of two atoms at ultra low temperatures, and barrier penetration in the presence of a resonance for a Morse potential. A key ingredient of the method is to divide the radial range into partitions, and in each partition expand the solution of the L-S equation into a set of Chebyshev polynomials. The expansion is called "spectral" because it converges rapidly to high accuracy. Properties of the Chebyshev expansion, such as rapid convergence, are illustrated by means of a simple example.

I. INTRODUCTION

As stated in the textbook by Cummings, Laws, Redish and Cooney [1], "Physics is a process of learning about the physical world by finding ways to make sense of what we observe and measure. As the inspiring teacher Richard Feynman wrote, [2] "Progress in all of the natural sciences depends on this interaction between experiment and theory"."

An important tool required for carrying out this interaction is the solution of equations provided by a particular theory, in order to be able to compare its predictions with experiment. As the equations become more and more involved, such as in global climate study, in the construction of pharmaceutical drugs, in the analysis of large organic chains that exist in live cells, in the understanding of superconductivity, in the tracing of the earth's interior by means of seismic waves, in the construction of devices that transmit digital information, in the study of atomic, nuclear and particle theory (particularly in lattice gauge theory), etc., the resort to numerical computational methods becomes increasingly more necessary.

The purpose of this paper is to point out special physical situations that require very accurate numerical algorithms, and to describe one such algorithm that has been recently developed. These special cases require either the evaluation of the solution of a wave equation out to large distances, or require high accuracy even for small distances, or both. Examples are the collision between atoms at extremely low temperatures. The understanding of such collisions is important for astro-physical applications, for the description of the state of atoms or molecules called Bose-Einstein condensates, and for the understanding of superfluidity in liquids formed out of weakly interacting atoms, such as the atoms of Helium. Helium is a "noble gas", i.e., its atoms interact mainly repulsively at short distances, yet, at intermediate distances (between 5 and 200 atomic units of distance) there is a small attractive valley in the potential energy curve (of a depth less than 3.5×10^{-3} atomic units of energy) within which a bound state can form. That weak attraction is in turn important for the molecular binding of a system of three or more helium atoms [3], [4]. The quantum mechanical wave function for the di-atom, in view of the weak binding energy of 4.4×10^{-9} atomic units of energy [5], extends to such large distances that accurate numerical values out to 2000 atomic units are required.

For the case of the radial, one-dimensional, Schrödinger equation

$$(d^2/dr^2 + k^2) \psi = V \psi, \tag{1}$$

where k is the wave number in units of inverse length and $V(r)$ is the potential in units of inverse length squared which contains the $L(L + 1)/r^2$ singularity, the most suitable equivalent integral equation for the S-IEM method is the Lippman-Schwinger equation

$$\psi(r) = \sin(kr) + \int_0^T \mathcal{G}_0(r, r') V(r') \psi(r') dr', \quad (2)$$

where \mathcal{G}_0 is the undistorted Green's function. In configuration space \mathcal{G}_0 has the well known semi-separable form $\mathcal{G}_0 = -(1/k) \sin(kr_<) \cos(kr_>)$. (for negative energies one would have $-(1/\kappa) \sinh(\kappa r_<) \exp(-\kappa r_>)$). By introducing the integral operator \mathcal{K}_T , so that when applied on a function $\psi(r)$ the result is

$$\mathcal{K}_T \psi(r) \equiv -\frac{1}{k} \cos(kr) \int_0^r dr' \sin(kr') V(r') \psi(r') - \frac{1}{k} \sin(kr) \int_r^T dr' \cos(kr') V(r') \psi(r'), \quad (3)$$

then Eq. (2) can be written as

$$\psi(r) = \sin(kr) + \mathcal{K}_T \psi(r), \quad (4)$$

where $\mathcal{K}_T \psi$ means that $\psi(r')$ is included in the integrands contained in Eq. (3). This form of Eq. (4) leads to the boundary condition that $\psi(0) = 0$, and since it assumes that for $r \geq T$ the potential $V(r) = 0$, it leads to the asymptotic behavior $\psi(r) = \sin(kr) + B \cos(kr)$, where B is a constant determined from the solution of Eq. (2). If $V(r) \neq 0$ for $r \geq T$, then matching at $r = T$ to the corresponding long range functions (Bessel or Coulomb, for example) is required, as is explained in Ref. ([6], [7]).

A new method for solving the Lippman-Schwinger integral equation (2), associated with the differential Schrödinger equation (1), has been developed recently [6] as an extension of a method due to Greengard and Rokhlin [8]. This method, to be called IEM (for integral equation method) has an accuracy which, for the same number of mesh-points, is far superior to the accuracy provided by finite difference methods for solving either an integral or a differential equation. One of the intended applications [9] is the solution of the Faddeev equations for a three-body system in configuration space, since it requires the calculation of wave functions out to large distances. It is the purpose of this paper to describe the application of this method for positive energy, two-body scattering cases, and compare it with several other methods. The application of this method to finding bound-state negative energies is being developed, with the intention of obtaining the He-He bound state described

above. The basic idea of the IEM is to divide the radial interval into partitions, obtain two special solutions of the restricted Lippman-Schwinger equation in each partition, called $Y(r)$ and $Z(r)$, by expanding these solutions into a set of Chebyshev polynomials, and calculating the coefficients of the expansion in each partition. That expansion is "spectral", i.e., it converges rapidly once the number of terms exceeds a certain value, and the error of truncating the expansion beyond that value is known, as is further explained below. Once the functions Y and Z are obtained in each partition, then the global function ψ in that partition is expressed as a linear combination of the Y and Z . The coefficients of that combination are subsequently calculated by solving a matrix equation, which is sparse, as will be explained. Spectral expansions to solve integral equations, albeit using a rather different set-up, in particular not using Green's functions or partitions, has also recently been developed by B. Mihaila [10].

Even though it is known that the errors which arise in the numerical solution of an integral equation are smaller than the errors in the solution of an equivalent differential equation, it is customary to solve the latter. The reason is that the algorithms for solving a differential equation by means of finite difference methods (such as Numerov or Runge-Kutta) are simple and do not require extensive storage space. By contrast, the discretization of an integral equation usually leads to large non-sparse matrices, and hence requires large investments of computer time and storage space. Therefore the gain in accuracy of the integral equation formulation is normally offset by a manifold increase in computational time. Our method circumvents this problem, as is described below. Before applications to physical cases are described, it is instructive to understand the basic accuracy properties of the spectral expansion method, as well as the basic ingredients of the IEM.

II. SPECTRAL EXPANSION

The main feature of a spectral expansion, namely its rapid convergence, will now be demonstrated by means of a simple example even though extensive discussions exist in the literature [11]. For the spectral expansion functions we will use Chebyshev polynomials only, although other orthogonal polynomials, such as Legendre, are also often used. We use Chebyshev polynomials because they are particularly well suited for obtaining the antiderivatives that appear in Eq. (3).

Spectral accuracy is described as follows: If a function $f(x)$, $-1 \leq x \leq 1$ is expanded in terms of Chebyshev polynomials $T_j(x)$,

$$f(x) = \frac{a_0}{2} + \sum_{j=1}^{\infty} a_j T_j(x) \quad (5)$$

then the error in truncating the expansion after n terms is proportional to $(n+1)^{-p}$, where p is the number of continuous derivatives which the function f has in the interval $-1 < x < 1$. Furthermore, this truncation error is also proportional to the $(n+1)$ 'th coefficient of the expansion, which means that, after a certain number of terms, the coefficients a_j decrease rapidly with j according to the same law j^{-p} . In particular, if $f(x)$ is infinitely differentiable, then the coefficients a_i converge to zero asymptotically faster than any fixed power of $(1/j)$. Hence the term ‘‘spectral convergence’’ is also referred to as ‘‘superalgebraic convergence’’.

These properties will now be illustrated by expanding the function $f(x) = \exp(x)$ into Chebyshev polynomials. The coefficients a_j in Eq. (5) are given by

$$a_j = \frac{2}{\pi} \int_{-1}^1 e^x T_j(x) (1-x^2)^{-1/2} dx = \frac{2}{\pi} \int_0^\pi e^{\cos \theta} \cos(j\theta) d\theta, \quad (6)$$

which follows from the orthogonality relation

$$\begin{aligned} \int_{-1}^1 T_k(x) T_j(x) (1-x^2)^{1/2} dx &= 0 \quad \text{if } j \neq k \\ &= \pi/2 \quad \text{if } j = k \neq 0 \\ &= \pi \quad \text{if } j = k = 0. \end{aligned} \quad (7)$$

The integral in Eq. (6) can be calculated analytically. In view of Eq. (6.9.19) in Ref. [12] the result is $a_j = 2I_j(1)$, where $I_j(z)$ is a modified Bessel function of order j . Using the asymptotic expansion for large orders of a Bessel function, Eq. (9.3.1) of Ref. [12], an approximation to a_j for large values of the index j is

$$a_j \simeq \frac{2}{\sqrt{2\pi j}} \left(\frac{e}{2j} \right)^j; \quad j \rightarrow \infty \quad (8)$$

Equation (8) shows that the value of a_j decreases with j faster than any fixed power of j , as is also demonstrated in the Table I. . The first row lists the values of a_j for $j = 2, 4, 6, 8$ as calculated from Eq. (6), (the results for the odd values of j are not shown) and the second row gives the values obtained from the asymptotic approximation (8) The table shows that

	a_2	a_4	a_6	a_8
Eq.(6)	$2.715E - 1$	$5.474E - 3$	$4.450E - 5$	$1.992E - 7$
Eq.(8)	$2.60E - 1$	$5.32E - 3$	$4.40E - 5$	$1.958E - 7$

TABLE I: Chebyshev expansion coefficients $a(k)$ of $f(x)=\exp(x)$

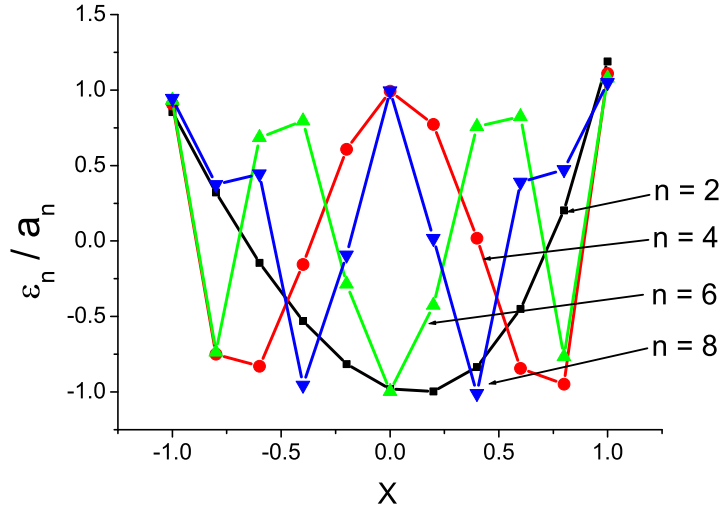


FIG. 1: Truncation errors in the expansion of $f(x) = \exp(x)$ into Chebyshev polynomials, divided by the first expansion coefficient not included in the sum.

the coefficients decrease rapidly with the order j . Will the truncation error also decrease rapidly?

The truncation error in the expansion is defined as $\epsilon_n(x) = f(x) - f_n(x)$ where $f_n(x)$ denotes the sum in Eq. (5) that is taken from $j = 1$ to $j_{\max} = n - 1$. A useful property of spectral expansions is that this error decreases with n proportionally to a_n , the first expansion coefficient not included in the sum. This is demonstrated in Fig. 1, which shows the ratio $\epsilon_n(x)/a_n$, for $n = 2, 4, 6$ and 8 . The figure shows that the curves are approximately contained between ± 1 , i.e., the truncation error is of the same magnitude as a_n independently of the value of x . Hence the truncation error does not show a Gibbs phenomenon at the end points, as would be the case for an expansion into a Fourier Series.

The above mentioned relation between the truncation error and the value of the Chebyshev coefficient provides a convenient method for finding the appropriate size of each parti-

tion, compatible with the overall prescribed error. Clenshaw and Curtis [13], who originated this spectral integration technique, recommend using the average size of the three last consecutive coefficients as an accuracy criterion.

Once the coefficients a_i of the expansion (5) are known for $j = 0, 1, \dots, N$, then one has a semi-analytical approximation to the function $f(x)$, given by the truncated form of Eq. (5)

$$f_N(x) = \frac{a_0}{2} + \sum_{j=1}^N a_j T_j(x), \quad (9)$$

that enables one to evaluate f_N at any point x in the interval $[-1, +1]$ without the need to carry out interpolations. A method for obtaining the coefficients a_j that does not require to evaluate the integrals in Eq. (6) is described in Ref. [13]. It consists in considering the $N + 1$ zeros ξ_α of T_{N+1} for $\alpha = 0, 1, \dots, N$, evaluating the expansion (9) at $x = \xi_\alpha$ for $\alpha = 0, 1, \dots, N$ and thus obtaining a set of $N + 1$ linear equations for the coefficients a_j . The matrix involved that relates the column vector of the $f(\xi_\alpha)$ to the vector of the a_j has elements formed from the values $T_j(\xi_\alpha)$, with $j, \alpha = 0, 1, \dots, N$. Details can be found in Ref. [6] and in textbooks. This is the method used to construct Tables II-IV.

The Chebyshev expansion is particularly suited to obtain the integral $\int_{-1}^x f_N(x') dx'$ of the function f_N without significant loss of accuracy. An expansion of this antiderivative function in terms of Chebyshev polynomials

$$F_N(x) = \int_{-1}^x f_N(x') dx' = \sum_{j=0}^{N+1} b_j T_j(x). \quad (10)$$

has the property that the coefficients b_j can be easily obtained in terms of the coefficients a_j , by means of a matrix usually denoted as S_L , as is described in textbooks as well as in Ref. [6]. The basic reason is that the integral from -1 to x of a particular T_j is given by a linear combination of $T_i(x)$ with $i \leq j + 1$. For example, $\int_{-1}^x T_2(x') dx' = [T_3(x) - 3T_1(x) - 2T_0(x)]/6$, and $\int_{-1}^x T_3(x') dx' = [T_4(x) - 2T_2(x) + T_0(x)]/8$. The sum in Eq. (10) should rigorously go to the upper limit $N + 1$. However, in numerical calculations the $(N + 1)$ 'th term is generally ignored. A similar matrix, called S_R , exists in order to obtain a Chebyshev expansion of $\int_x^1 f_N(x') dx'$. A numerical verification that the accuracy of the antiderivative is of the same order of magnitude as the accuracy of the expansion of the function f_N , again for $f(x) = \exp(x)$, is shown in the second and third columns of Table II.

The derivatives with respect to x of f_N can also be obtained via Chebyshev expansions, but in order to maintain a prescribed accuracy, the truncation value N has to be increased

x	$F_N - e^x + e^{-1}$	$f_N - e^x$	$f_N^{(1)} - e^x$	$f_N^{(2)} - e^x$
-0.8	.25(-11)	-.51(-9)	.12(-8)	.14(-6)
-0.6	.11(-8)	.51(-9)	.10(-8)	-.81(-7)
-0.4	.29(-9)	-.30(-9)	-.48(-8)	.37(-7)
-0.2	.27(-9)	-.23(-9)	.49(-8)	.24(-7)
0.0	.11(-8)	-.55(-9)	.50(-10)	-.55(-7)
0.2	.37(-9)	-.24(-9)	-.52(-8)	.23(-7)
0.4	.20(-9)	-.32(-9)	.51(-8)	.41(-7)
0.6	.11(-8)	.57(-9)	-.10(-8)	-.91(-7)
0.8	.21(-10)	-.58(-9)	-.15(-8)	.16(-6)

TABLE II: Coefficients a_j and $a_j \times j^2$ for the expansion of $\exp(x)$ for $N = 9$

j	7	8	9	10	11
a_j	.32(-5)	.20(-6)	.11(-7)	.55(-9)	.25(-10)
$a_j \times j^2$.16(-3)	.13(-4)	.88(-6)	.55(-7)	.30(-8)

TABLE III: Coefficients a_j and $a_j \times j^2$ for the expansion of $\exp(x)$

accordingly. Call $f_N^{(1)} = df_N/dx$, $f_N^{(2)} = d^2f_N/dx^2$, etc. One of two methods consists in taking the derivatives of the Chebyshev polynomials term by term in Eq. (9)

$$f_N^{(n)}(x) = \sum_{j=1}^N a_j T_j^{(n)}(x), \quad n = 1, 2, \dots \quad (11)$$

The expressions for $T_j^{(n)}(x)$ can be given analytically, and hence $f_N^{(n)}$ can be evaluated numerically at any point x in $[-1, +1]$. By taking a derivative of a polynomial of order j , the result is a polynomial of order $j - 1$, whose magnitude is of order j times the original polynomial. For example, $d^2T_j(x)/dx^2 = [xdT_j/dx - j^2T_j]/(1 - x^2)$. That leads one to expect that the errors in Table II for a derivative of order n are related to the coefficient of the next to the last Chebyshev polynomial, (T_{N+1}) times $(N + 1)^n$. Table III lists coefficients a_i and $a_j \times j^2$ and by comparing Tables II and III one sees that this expectation is borne out.

A second method consists in writing a Chebyshev expansion for df/dx

$$df_N/dx = \frac{c_0}{2} + \sum_{j=1}^{N-1} c_j T_j(x), \quad (12)$$

x	$F_N - e^x + e^{-1}$	$f_N - e^x$	$f_N^{(1)} - e^x$	$f_N^{(2)} - e^x$
-0.8	.29(-14)	.72(-15)	.24(-14)	-.44(-12)
-0.6	.36(-15)	.33(-15)	.21(-13)	.12(-12)
-0.4	.31(-14)	.44(-15)	-.32(-13)	-.15(-12)
-0.2	-.56(-16)	-.22(-14)	.29(-13)	.37(-12)
0.0	.33(-14)	.48(-14)	-.11(-13)	-.57(-12)
0.2	..11(-15)	-.40(-14)	-.21(-13)	.57(-12)
0.4	.24(-14)	.20(-14)	.44(-13)	-.37(-12)
0.6	.67(-15)	0	-.42(-13)	.25(-12)
0.8	.29(-14)	.88(-15)	.19(-13)	-.69(-12)

TABLE IV: Same as Table II. for $N = 13$

and by noting that the expansion coefficients c_j are related to the coefficients a_j in Eq. (9) as follows: $c_{N-1} = 2Na_N$, $c_{N-2} = 2(N-1)a_{n-1}$, and for $j \leq N-2$, $c_{j-1} = c_{j+1} + 2ja_j$. The error in df_N/dx is approximately equal to the magnitude of c_N , that in turn permits one to determine the value of N from the relation $c_N = 2(N+1)a_{N+1}$

In the numerical example given in this section the upper value N of the sums in the Chebyshev expansions was taken as $N = 9$. However, in the numerical solution of the integral equation, as described in the next section, $N = 15$. This leads to accuracies of the order of 10^{-14} , as is discussed in the realistic numerical examples described below. In order to demonstrate the rapid gain in accuracy for a small increase in the value of N , we show errors similar to those displayed in Table II, for $N = 13$. The accuracy increases approximately by four or five orders of magnitude as N is increased from 9 to 13.

Once the coefficients of a Chebyshev expansion (9) of a function $f_N(x)$ are obtained, the Fourier components $\int_{-1}^{+1} f(x) \sin(ax) dx$ and $\int_{-1}^{+1} f(x) \cos(ax) dx$ of that function can also be obtained, as follows. If the coefficients d_k of the expansion of the function

$$f(x) \sin(ax) = \sum_{k=0}^M d_k T_k(x) \quad (13)$$

are known, then the integrals $\int_{-1}^{+1} f(x) \sin(ax) dx$ can be easily obtained by applying the matrix S_L described above upon the row vector of the coefficients d_k , and remembering that

$T_k(1) = 1$. In order to obtain the coefficients d_k one requires the integral

$$\int_{-1}^{+1} T_k(x) f(x) \frac{\sin(ax)}{\sqrt{1-x^2}} dx = \sum_j a_j \int_{-1}^{+1} T_k(x) \frac{\sin(ax)}{\sqrt{1-x^2}} T_j(x) dx, \quad (14)$$

in view of Eqs. (7). By using the relation

$$2T_k(x)T_j(x) = T_{k+j}(x) + T_{|k-j|}(x) \quad (15)$$

the integrals on the right hand side of Eq. (14) can be carried out analytically in terms of Bessel J functions by using the expression [14]

$$\int_{-1}^1 T_{2n+1}(x) \frac{\sin(ax)}{\sqrt{1-x^2}} dx = (-1)^n \pi J_{2n+1}(a). \quad (16)$$

For Chebyshev polynomials of even order the above integrals vanish. Similarly, one can obtain the coefficients of the Chebyshev expansion of $f_N(x) \cos(ax)$ by making use of [14]

$$\int_{-1}^1 T_{2n}(x) \frac{\cos(ax)}{\sqrt{1-x^2}} dx = (-1)^n \pi J_{2n}(a) \quad (17)$$

In this manner the loss of accuracy in the integrals above that takes place for large values of a can be avoided.

Finally, we remark that the Chebyshev expansions can be used on any interval $[a, b]$ by means of the linear transformation

$$x = \frac{2}{b-a}r - \frac{b+a}{b-a} \quad (18)$$

that maps $r \in [a, b]$ into $x \in [-1, 1]$.

III. THE INTEGRAL EQUATION METHOD

Our method for solving the Lippman-Schwinger equation (2) is described below for the case of one channel and positive energy. The boundary conditions, and hence the choice of the Green's function, is appropriate for a scattering situation. Beyond a large radial distance called T the potential other than the centripetal or Coulomb potentials is set to zero. The radial interval $[0, T]$ is partitioned into subintervals i , with $i = 1, 2, \dots, M$. The lower and upper boundaries of interval i are b_{i-1} and b_i , respectively, with $b_M = T$. In each partition the integral operator \mathcal{K}_i is defined

$$\mathcal{K}_i = -\frac{1}{k} \cos(kr) \int_{b_{i-1}}^r dr' \sin(kr') V(r') - \frac{1}{k} \sin(kr) \int_r^{b_i} dr' \cos(kr') V(r'), \quad b_{i-1} \leq r \leq b_i. \quad (19)$$

This operator is similar to \mathcal{K}_T defined in Eq. (3), with the exception that the upper and lower limits of the integration are b_{i-1} and b_i . Two independent local solutions $Y_i(r)$ and $Z_i(r)$ in partition i are obtained by solving the integral equation locally, driven by two different functions $\sin(kr)$ and $\cos(kr)$,

$$\begin{aligned} (1 - \mathcal{K}_i)Y_i &= \sin(kr); & b_{i-1} \leq r \leq b_i \\ (1 - \mathcal{K}_i)Z_i &= \cos(kr); & b_{i-1} \leq r \leq b_i. \end{aligned} \quad (20)$$

It is important to note that boundary conditions are not needed to make the solutions of Eqs. (20) unique, unless the operator $(1 - \mathcal{K}_i)$ has zero eigenvalues. This situation is of course different from the solutions of the differential equation (1), since the functions $\sin(kr)$ and $\cos(kr)$ are eigenvectors of the operator $(d^2/dr^2 + k^2)$ corresponding to zero eigenvalue. If accidentally the operator $(1 - \mathcal{K}_i)$ has a zero eigenvalue in a particular partition, then by decreasing the size of the partition the zero eigenvalue should disappear because the "size" of \mathcal{K}_i decreases correspondingly. Another advantage of the integral equation method over the differential equation method is that the operator \mathcal{K}_i is compact, while the operator $(d^2/dr^2 + k^2)$ is not. A compact operator can be approximated to ever increasing accuracy by a separable expansion of basis vectors, and hence a numerical representation (or discretization) of the operator is numerically stable.

The values of the functions Y and Z and their derivatives at the boundary points of the partition i can be obtained from Eqs. (20) by inserting into Eq. (19) for r the value b_{i-1} or b_i , respectively. By defining the dimensionless quantities

$$\begin{aligned} (GY)_i &= \frac{1}{k} \int_{b_{i-1}}^{b_i} \cos(kr)V(r)Y_i(r)dr ; & (FY)_i &= \frac{1}{k} \int_{b_{i-1}}^{b_i} \sin(kr)V(r)Y_i(r)dr \\ (GZ)_i &= \frac{1}{k} \int_{b_{i-1}}^{b_i} \cos(kr)V(r)Z_i(r)dr ; & (FZ)_i &= \frac{1}{k} \int_{b_{i-1}}^{b_i} \sin(kr)V(r)Z_i(r)dr \end{aligned} \quad (21)$$

one obtains

$$\begin{aligned} Y_i(b_{i-1}) &= \sin(kb_{i-1})[1 - (GY)_i] \\ Y'_i(b_{i-1}) &= k \cos(kb_{i-1})[1 - (GY)_i] \\ Z_i(b_{i-1}) &= \cos(kb_{i-1}) - \sin(kb_{i-1})(GZ)_i \\ Z'_i(b_{i-1}) &= -k[\sin(kb_{i-1}) + \cos(kb_{i-1})(GZ)_i] \end{aligned} \quad (22)$$

and

$$\begin{aligned}
Y_i(b_i) &= \sin(kb_i) - \cos(kb_i)(FY)_i \\
Y'_i(b_i) &= k[\cos(kb_i) + \sin(kb_i)(FY)_i] \\
Z_i(b_i) &= \cos(kb_i)[1 - (FZ)_i] \\
Z'_i(b_{i-1}) &= -k \sin(kb_{i-1})[1 - (FZ)_i].
\end{aligned} \tag{23}$$

In the above, a prime indicates a derivative with respect to r . Since the functions Y and Z obey the Schrödinger equation (1), the wronskian of these functions, $W(Y, Z) = Y'Z - YZ'$, is independent of the point r within the interval i if V is a local potential. Using the Eqs. (22) and (23) one can express the wronskian at $r = b_{i-1}$ and $r = b_i$, respectively, in terms of the overlap integrals defined in Eq. (21). One obtains

$$\begin{aligned}
W(Y, Z)_{b_{i-1}} &= k[1 - (GY)_i] \\
W(Y, Z)_{b_i} &= k[1 - (FZ)_i],
\end{aligned} \tag{24}$$

which implies in particular that

$$(GY)_i = (FZ)_i. \tag{25}$$

This result also shows that if (GY) becomes close to unity in a particular partition, then the functions Y and Z will no longer be significantly linearly independent of each other, and the IEM method becomes unreliable in this partition. The remedy is to decrease the length of the partition, since the value of (GY) will then also decrease.

The solution of Eqs. (20) in each interval i is accomplished by expanding these functions in terms of Chebyshev Polynomials, and solving the matrix equations for the corresponding coefficients. The procedure is well described in Ref. [6], and will not be repeated here. However, a few remarks are in order: 1. The coefficients of the expansion of the functions $Y_i(r)$ and $Z_i(r)$ in terms of the Chebyshev polynomials are obtained with high spectral accuracy by using Chebyshev collocation points in each partition, together with the Curtis-Clenshaw quadrature [13]. 2. The Eqs. (20) are not the inverse of the Schrödinger Eq., otherwise there would be no gain in accuracy in using the integral equation. 3. The inverse of the operator $(1 - \mathcal{K}_i)$ always exists if the partition i is made small enough, because then the operator \mathcal{K}_i becomes small in comparison to the unit operator 1. 4. The calculation of the functions $Y_i(r)$ and $Z_i(r)$ is not computationally expensive, because the number of

collocation points in each partition is prescribed to be small (16, usually), and hence the matrices involved, although not sparse, are of small size (e.g. 16×16). 5. The accuracy of the calculation of the functions $Y_i(r)$ and $Z_i(r)$ can be prescribed ahead of time by examining the magnitude of the last three coefficients of the expansions. If they are not smaller than the prescribed accuracy, then the size of the partition is reduced by a factor of two, and the accuracy will increase correspondingly. This adjustment of partition sizes can be done automatically, as is demonstrated in detail in Ref [15].

Next the calculation of the global function $\psi(r)$ in each partition i is described. Since the functions $Y_i(r)$ and $Z_i(r)$ are linearly independent solutions of the Schrödinger equation (1), and since the latter is a linear equation, the function $\psi(r)$ can be expressed as a linear combination of these two functions

$$\psi(r) = A_i Y_i(r) + B_i Z_i(r), \quad b_{i-1} \leq r \leq b_i. \quad (26)$$

A relationship between the coefficients A and B in one particular partition i and those in the other partitions can be obtained by returning to the original Lippman-Schwinger Eq. (2) for the function $\psi(r)$, with r contained in that particular partition i . By expressing the integrals in Eq. (4) as sums over the integrals over all partitions, by inserting for $\psi(r)$ the expression (26) for every partition, and by making use of Eqs. (20), one obtains

$$A_i = 1 - \sum_{j=i+1}^M [(GY)_j A_j + (GZ)_j B_j], \quad i = 1, 2, \dots, M \quad (27)$$

and

$$B_i = - \sum_{j=1}^{i-1} [(FY)_j A_j + (FZ)_j B_j], \quad i = 1, 2, \dots, M. \quad (28)$$

The 1 appears in Eq. (27) and not in Eq. (28) because the "driving term" in Eq. (2) is $\sin(kr)$ and not $\cos(kr)$. When $i = 1$ then the sum in Eq. (28) is set to zero, which requires that $B_1 = 0$. That requirement is compatible with the condition that $\psi(0) = 0$, since $Z_1(0) \neq 0$ and $Y_1(0) = 0$.

The equations (27) and (28) can be manipulated in several different ways so as to increase the sparseness of the matrices that define the solutions A_i and B_i . One way, described in Refs. [6] and [7], is to subtract from each other Eqs. (27) for consecutive values of i , and similarly for Eqs. (28). By defining the column vectors

$$\alpha_i = \begin{pmatrix} A_i \\ B_i \end{pmatrix}; \quad \omega = \begin{pmatrix} 1 \\ 0 \end{pmatrix}; \quad \zeta = \begin{pmatrix} 0 \\ 0 \end{pmatrix} \quad (29)$$

one obtains

$$\begin{pmatrix} \mathbf{I} & \mathbf{M}_{12} & & & & \mathbf{0} \\ \mathbf{M}_{21} & \mathbf{I} & \mathbf{M}_{23} & & & \\ & \mathbf{M}_{32} & \mathbf{I} & \mathbf{M}_{34} & & \dots \\ & & & & & \\ & & & & \mathbf{M}_{M-1,M-2} & \mathbf{I} & \mathbf{M}_{M-1,M} \\ \mathbf{0} & & & & & \mathbf{M}_{M,M-1} & \mathbf{I} \end{pmatrix} \begin{pmatrix} \alpha_1 \\ \alpha_2 \\ \alpha_3 \\ \dots \\ \alpha_{M-1} \\ \alpha_M \end{pmatrix} = \begin{pmatrix} \zeta \\ \zeta \\ \zeta \\ \dots \\ \zeta \\ \omega \end{pmatrix} \quad (30)$$

where \mathbf{I} and $\mathbf{0}$ are two by two unit and zero matrices, respectively, and where

$$\mathbf{M}_{i-1,i} = \begin{pmatrix} (GY)_i - 1 & (GZ)_i \\ 0 & 0 \end{pmatrix}, \quad i = 2, 3, \dots, M \quad (31)$$

and

$$\mathbf{M}_{i,i-1} = \begin{pmatrix} 0 & 0 \\ (FY)_{i-1} & (GZ)_{i-1} - 1 \end{pmatrix}, \quad i = 2, 3, \dots, M. \quad (32)$$

Note that Eq. (30) generally connects the A and B 's of *three* contiguous partitions. For example, $M_{21}\alpha_1 + \alpha_2 + M_{23}\alpha_3 = \zeta$.

Another way of combining Eqs. (27 and 28) is to first write them into a (2×1) column form involving the vectors α_i , and subsequently subtracting equations with contiguous i -values from each other, however leaving the last equation in its original form. The result is [16]

$$\begin{pmatrix} \Gamma_1 & -\Omega_2 & & & & \\ & \Gamma_2 & -\Omega_3 & & & \\ & & \Gamma_3 & -\Omega_4 & & \dots \\ & & & & & \\ & & & & \Gamma_{M-1} & -\Omega_M \\ \gamma_1 & \gamma_2 & \gamma_3 & \dots & \gamma_{M-1} & \mathbf{I} \end{pmatrix} \begin{pmatrix} \alpha_1 \\ \alpha_2 \\ \alpha_3 \\ \dots \\ \alpha_{M-1} \\ \alpha_M \end{pmatrix} = \begin{pmatrix} \zeta \\ \zeta \\ \zeta \\ \dots \\ \zeta \\ \omega \end{pmatrix}, \quad (33)$$

where

$$\Gamma_i = \begin{pmatrix} 1 & 0 \\ -(FY)_i & 1 - (FZ)_i \end{pmatrix}, \quad (34)$$

$$\Omega_i = \begin{pmatrix} 1 - (GY)_i & -(GZ)_i \\ 0 & 1 \end{pmatrix}, \quad (35)$$

and

$$\gamma_i = \begin{pmatrix} 0 & 0 \\ (FY)_i & (FZ)_i \end{pmatrix}. \quad (36)$$

It is noteworthy that the first $M - 1$ equations in (33),

$$\Gamma_i \alpha_i = \Omega_{i+1} \alpha_{i+1}, \quad i = 1, 2, \dots, M - 1 \quad (37)$$

are equivalent to matching the wave function ψ at the end of partition i to ψ at the start of partition $i + 1$. This can be seen by imposing the two conditions $\psi_i(b_i) = \psi_{i+1}(b_i)$ and $\psi'_i(b_i) = \psi'_{i+1}(b_i)$ where ψ_i is the wave function in partition i given by Eq. (26) and where ψ'_i is the corresponding derivative. Inserting into Eq. (26) the values of Y_i and Z_i or their derivatives at either the beginning or the end of a partition as given by Eqs. (22) or (23), respectively, one obtains the result

$$\begin{aligned} A_i &= A_{i+1}[1 - (GY)_{i+1}] - B_{i+1}(GZ)_{i+1} \\ B_{i+1} &= -A_i(FY)_i + B_i[1 - (FZ)_i]. \end{aligned}$$

These two equations are equivalent to Eq. (37) .

By successive applications of Eq. (37)

$$\alpha_{i+1} = (\Omega_{i+1})^{-1} \Gamma_i \alpha_i$$

one can relate the values of α_i , $i = 2, 3, \dots, M$, to α_1 and then use the last of the (33) equations

$$\sum_{i=1}^{M-1} \gamma_i \alpha_i + \alpha_M = \begin{pmatrix} 1 \\ 0 \end{pmatrix} \quad (38)$$

in order to find the value of A_1 . It can be shown that Eq. (38) is compatible with the requirement that $B_1 = 0$.

Several comments are in order.

a) The "big" matrices in Eqs. (33) or (30) are sparse, and can be solved by Gaussian elimination. Since the number of floating point operations (flops) is of order M , the computational complexity of the S-IEM is comparable to that of the solution of the differential equation. This sparseness property results from the semi-separable nature of the integration kernel \mathcal{K} , as is shown in Refs. [6], [7], which however applies only in the configuration representation of the Green's function. This part of our procedure also differs substantially from that of

Ref. [8].

b) The scattering boundary conditions can be implemented reliably. This is because the Greens function incorporates the asymptotic boundary conditions automatically. However, in the coupled channel case for angular momentum numbers $L > 0$, the coupled equations have to be solved as many times as there are open channels because our Green's functions are composed of $\sin(kr)$ and $\cos(kr)$, rather than of Riccati-Bessel functions. We show [7] that the desired linear combination of the solutions can be obtained without appreciable loss of accuracy, since the matrix required in the solution for the coefficients has a condition number not much larger than unity. This means that our various solutions are linearly independent to a high degree, contrary to what can be the case with the solution of differential equations.

c) The method is very economical in the total number of mesh-points required in the interval $[0, T]$ because in each partition or spectral collocation method requires very few mesh points (like in the case of Gauss-Legendre integration as compared to Simpson' integration), and the required length of each partition can be easily adjusted to optimal size based on the magnitude of the coefficients of the expansion of the functions Y and Z into Chebyshev polynomials, as described before.

d) The calculation can be distributed onto parallel processors. This is because the functions Y and Z , as well as the overlap integrals (21), required for Eqs. (33) or (30), can be calculated separately for each partition independently of the other ones. This is an important point, since if the number of channels increases, the number of the quantities (21) increases accordingly.

Property c) is also important because, due to the small number of total mesh-points, the accumulation of machine round-off errors is correspondingly small. In addition, as is well known, integration is numerically more stable than differentiation as discussed for example in sections 4.4 and 5.2 on pages 203 and 263, respectively, in Ref. [17], and is also shown in Tables II and IV. Hence the accumulation of the inherent round-off error is smaller for the numerical solution of an integral equation than for the numerical solution of differential equations. The small accumulation of roundoff errors in comparison to a finite difference method is clearly illustrated in Fig. 1 of Ref. [6], which compares the round off errors in the solution of Bessel's equation obtained via the IEM with that of the Numerov method.

IV. APPLICATIONS

The various features of the S-IEM method will now be illustrated by means of examples. The spectral property that high accuracy is reached very rapidly (in principle faster than any inverse power of the number of mesh-point in a given radial interval) is illustrated for the case of the scattering of an electron from an Hydrogen atom. This is a suitable example, because the identity between the incoming electron and the electron bound in the atom leads to an additional integral term in the Schrödinger equation, if the Pauli exclusion principle is implemented via the Hartree-Fock formulation. Rigorously including this term is difficult for the conventional finite difference methods, and various techniques were developed for that purpose [18], and additional references can be found in [19]. By contrast, in the IEM method this additional integral term is easily incorporated without substantial loss of accuracy [19], because the integral kernel is semi-separable. A comparison between the S-IEM and a conventional NIEM method [20] is shown in Fig (2). The $L = 0$ singlet phase shift was calculated for the incident momentum $k = 0.2 (a_0)^{-1}$ and $T = 50 a_0$, while the target electron was kept in the ground state of the Hydrogen atom. The figure shows that, as the number m of partitions is increased, and accordingly the number of mesh-points $m \times 16$, the number of stable significant figures in the phase shift increases very rapidly for the S-IEM, illustrating the spectral nature of that method. By comparison, for a method employing finite difference techniques based on an equi-spaced set of mesh-points, the number of stable significant figures increases much more slowly [20] for solving a very similar integral equation non-iteratively by means of the NIEM method. Although it gives a good illustration of the numerical accuracy, this example is nevertheless not very realistic physically because the virtual excitations of the bound electron to the myriad of possible states, both bound and in the continuum, is not included. Inclusion of these excitations requires "state of the art" calculations that are presently in progress [21].

Another example is the scattering of atoms at ultra-low temperature. This information is needed for the investigation of photo association [22] of the two atoms into a molecule, and also in the formation of Bose-Einstein condensates (BE) [23]. The lifetime of a BE condensate is reduced [24] by the three-body process in which two of the atoms combine to form a molecule in the presence of a third atom, that in turn carries away the energy of formation of the dimer. The depletion rate is proportional to the fourth power of the scattering length. At

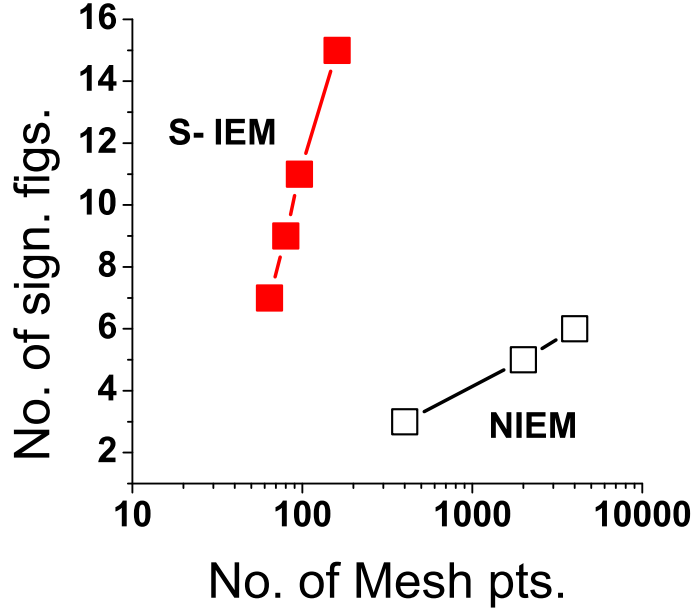


FIG. 2: Comparison of the numerical stability of two methods for calculating the singlet phase shift for electron-hydrogen scattering, as described in the text. The number of significant figures on the y-axis is the number of decimal places for which the result remains the same as the number of meshpoints is increased. S-IEM is the the spectral method described in this paper, and NIEM is a non-iterative method of solving the same integral equation carried out by Sams and Kouri.

low energies a stable method of calculation is required because, the lower the incident energy, the more the long-range part of the potentials contributes significantly to the phase shift. A bench mark calculation was performed using the S-IEM method, involving two channels, one closed and one open [15]. The numerical stability of the $L = 0$ scattering phase shift as a function of the number of mesh points used was investigated, and was compared with various other methods of calculation, and the results are shown in Fig. 3. In all of these calculations the maximum radius is $T = 500$ atomic units (a_0 or *Bohr*), the diagonal potentials are of the Lenard Jones form $C_6/r^6 + C_{12}/r^{12}$, and the coupling between the two channels is of an exponential form [15]. At small distances, due to the large depth of the potentials, the wave function oscillates rapidly, and hence it is important to be able to adjust the size of the partitions accordingly. Since no analytical exact comparison values exist, the "error" in the figure is defined as the absolute value of the difference between the result for a given value

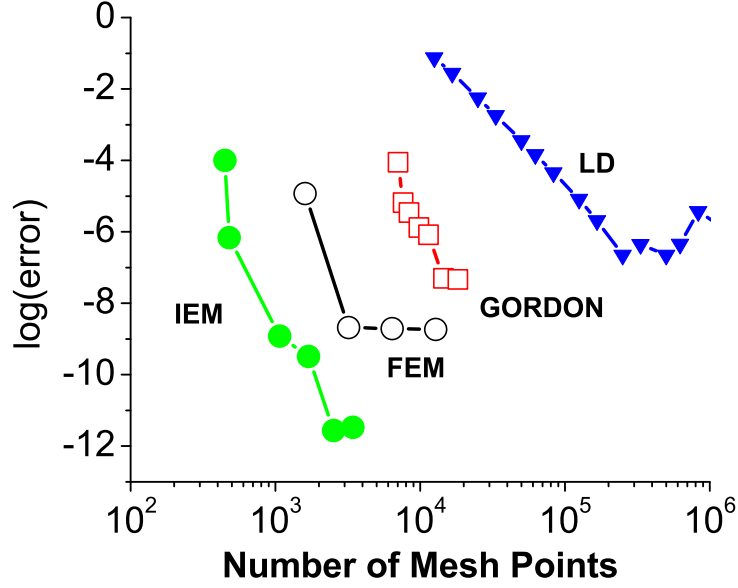


FIG. 3: Comparison of errors for various methods of computation of the $L = 0$ phase shift for cold atom collision, as a function of the number of mesh points in a fixed radial interval. IEM is the method described here, FEM is a finite element method, Gordon and LD (logarithmic derivative) are two finite difference methods, as explained in the text.

of the number of mesh points N and the maximum value of N employed in the particular method. The FEM method is a finite element method [25] implemented by B. D. Esry and carried out by J. P. Burke, Jr [15]; the Gordon method [26] was implemented by F. E. Mies [15], and LD is a logarithmic derivative method implemented by the code MOLSCAT [27], [28]. For the LD curve the roundoff errors apparently overwhelm the truncation errors when the number of mesh points is larger than 2×10^5 . The S-IEM again shows a rapid improvement of accuracy with the number of mesh-points, and it reaches a somewhat higher stability than the FEM. Our benchmark calculation was recently used [29] for comparison with a finite difference method in which the potential in each partition is assumed constant (similar to what is the case with one form of the Gordon method), and the corrections are taken into account iteratively.

In many quantum mechanical calculations, penetration of the wave function through a barrier is involved. Examples in nuclear physics are the alpha particle decay of a nucleus, or the fission of a nucleus into two daughter nuclei, or in the scattering of a nucleus by another

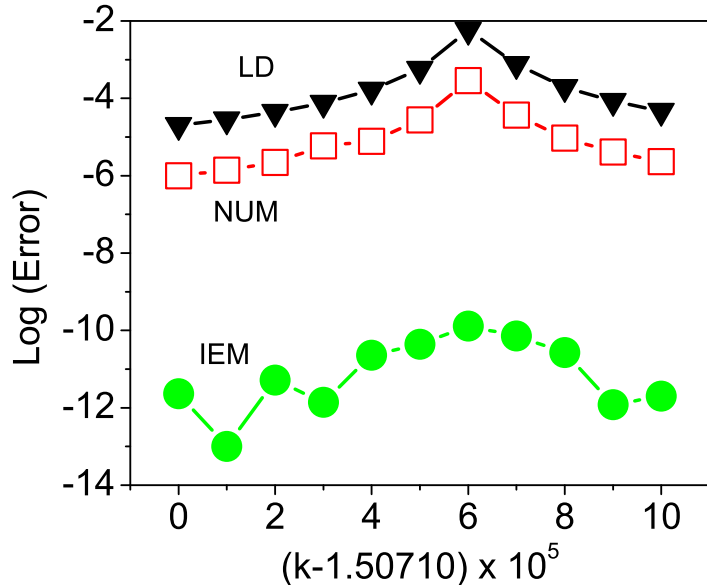


FIG. 4: Numerical error in the phase shift for scattering from a Morse potential with a barrier, in the region of a narrow resonance, as a function of the incident momentum. The error is obtained by comparison with the analytic result, the momentum closest to the resonance occurs for $k = 1.50716$.

nucleus, and also in many similar situations in atomic physics. A barrier frequently occurs when a long range repulsive potential, such as a centripetal potential of the form $L(L+1)/r^2$ or that of a repulsive Coulomb potential, is added to an attractive nuclear or atomic potential of a shorter range. For the scattering or the fusion reaction of a light nucleus with a heavy nucleus at low incident energies [30], [31] the penetration of the corresponding wave function through such a barrier can pose substantial calculational challenges [32]. In low temperature atom-molecule scattering, similar barrier penetration effects become crucial [33]. For this reason a test of the accuracy of a calculation for a case involving barrier penetration was performed. The potential chosen is an "inverted" form of the Morse potential [34] for which analytic results exist for the scattering phase shift [35]. It has an attractive negative valley near the origin at $r = 0$ followed by a smooth positive energy barrier, a situation which leads to resonances. For resonant energies the wave function in the valley region can become very large if the width of the resonance is sufficiently small, and in the barrier region this wave function *decreases* as a function of distance. This decrease of the wave function in the barrier region amplifies the numerical errors, since in this region the numerical errors tend to *increase*

exponentially. The accuracy of three methods of calculation for a particular resonance which occurs for an incident momentum k in the region $1.5071 fm^{-1} < k < 1.5072 fm^{-1}$ are illustrated in Fig. 4. The parameters of the Morse potential are given in Fig.10 of Ref. [35], the maximum amplitude of the wave function in the valley region at the resonance near $k = 1.50716 fm$, is close to 300 (asymptotically it is equal to 1). The error is defined as the difference between the analytical and the numerical results; the momenta k on the x-axis are given as the excess over the momentum at the left side of the resonance, $k = 1.50710 fm^{-1}$. The IEM curve is obtained with the method described in this paper, NUM is a sixth order Numerov method, also denoted as Milne's method [36], and the LD curve is obtained with the Logarithmic Derivative method, implemented by MOLSCAT [37]. The matching radius for the two finite difference methods, LD and NUM, was set at $50 fm$, and the corresponding analytical values were extrapolated from $T = \infty$ to $T = 50 fm$ by a Green's function iteration procedure described in Ref. [15], and are listed in Table 1 of Ref. [35]. For the more precise S-IEM calculation that extrapolation was not accurate enough, and $T = 100$ was used instead. One sees from the figure that the accuracy of the S-IEM is several order of magnitudes (six) higher than that of the Numerov method.

V. DISCUSSION AND CONCLUSIONS

A simple way to distinguish a spectral method from a finite difference method is that, in a particular partition, the mesh points in the former are not equi-spaced, while in the latter they are. Even though the accuracy of finite difference methods can be substantially increased by extrapolating the algorithms to equivalent zero-sized distance between mesh points [38], such extrapolation methods may become cumbersome. Our spectral S-IEM method is one of a class of well-known methods that divide the spatial domain into partitions (or sectors), and expand the solution on a suitable set of basis functions in each partition. One example is the method of Gordon [26], that uses Airy basis functions. The potential in each partition is approximated by a linear function, and the Airy functions are the corresponding exact solutions of the differential equation. This method was included among the comparisons carried out for the atom-atom scattering case, illustrated in Fig. 3. Gordon's method is widely used for atomic physics calculations, and one of the implementations can be found in Refs. [39] and [29]. This is a "potential following method" that

is particularly efficient when the potential varies slowly with distance. Another example is the method utilized by Light and Walker [40] in which the potential in each partition is approximated by a constant. In this case the Green's function that propagates the solution from one end of the partition to the other can be written simply in terms of sine and cosine functions. This method lends itself well to propagate the inverse of the logarithmic derivative of the solution from one end of a partition to the other end, without calculating the solution itself. This is called the R-matrix propagation method, and has been implemented by Burke and Noble [41]. This method, as implemented by the code MOLSCAT [27], was included among the comparisons carried out for the barrier penetration calculation, illustrated in Fig. 4. A "function following" method that expands the Greens function in a given partition in terms of Legendre Polynomials, without making approximations on the potentials, is given by Baluja *et al.* [42]. This method is also implemented in the computer code FARM [41]. The resulting expansion of the distorted Green's function $\mathcal{G}(r, r')$ is of a separable form, i.e., it is given as a sum over products of functions $u(r) \times v(r')$. A similar form is obtained by using Sturmian basis functions [43], [44]. However such expansions do not converge to high accuracy because the derivative of a Green's function has a discontinuity at the points $r = r'$. Our S-IEM method does not suffer from that difficulty because the distorted Green's function $\mathcal{G}(r, r')$ is obtained in terms of the exact undistorted Green's function $\mathcal{G}_0(r, r')$ through Eq. (20). The numerical solution of Eq. (20) is equivalent to expressing the distorted Green's function in terms of the undistorted one, according to

$$\mathcal{G} = (1 - \mathcal{G}_0 V)^{-1} \mathcal{G}_0,$$

and since \mathcal{G}_0 is given exactly in terms of its semi-separable form [near Eq. (2)] there is no loss of accuracy. The functions $Y(r)$ and $Z(r)$ are two independent solutions of both the Schrödinger equation and the Lippman-Schwinger equation in a particular partition, and they represent the two basis functions in terms of which the global solution is obtained in each partition. The equation (37), based on algebraic matrix Eq. (33), that relates the two expansion coefficients in one partition to the coefficients of *one* adjoining partition is equivalent to the propagation of the logarithmic derivative from one partition to the next. However, the method represented by Eq. (30) relates the coefficients in one partition to those in *two* other partitions appears not to be as closely related to the propagation of the logarithmic derivative, hence a comparison of the two methods for particular cases would

be very desirable. The method involving two adjoining partitions can be shown to be very similar to the multiple shooting method for solving two-point boundary value problems [45]. How the computational complexity scales with the number of coupled channels, in comparison with that of other methods, has also yet to be investigated.

In summary, a recently developed method for solving the Lippman-Schwinger integral equation is described and is applied to the solution of several physical problems. Since the new S-IEM is considerably more stable than finite difference methods, it is concluded that the S-IEM may become the method of choice for particular applications, such as atomic physics calculations that involving large distances, require high accuracy, and need to be carried out in configuration space.

-
- [1] K. Cummings, P. W. Laws, E. R. Redish and P. J. Cooney, *Understanding Physics*, (John Wiley & Sons, Inc, 2004) Vol. 1, p. 2;
 - [2] R. P. Feynman, *The Feynman Lectures on Physics*, Ch. 1. (Addison-Wesley, Reading, MA, 1964);
 - [3] T. Gonzalez-Lezana, J. Rubayo-Soneira, S. Miret-Artés, F. A. Gianturco, G. Delgado-Barrio, and P. Villarreal, *Efimov States for ^4He Trimers?*, Phys. Rev. Lett., **82**, 1648-1651 (1999);
 - [4] Cono. di Paola, Franco A. Gianturco, Gerardo Delgado-Barrio, Salvador Miret-Artés, and Pablo Villarreal, *The ^4He Trimer: Structure and Energetics of a Very Unusual Molecule*, Collect Czech. Chem. Commun., **68**, 1-22 (2003);
 - [5] K. T. Tang, J. P. Toennies, and C. L. Yiu, *Accurate Analytical He-He van der Waals Potential Based on Perturbation Theory*, Phys. Rev. Lett. **74**, 1546-1549 (1995);
 - [6] R. A. Gonzales, J. Eisert, I Koltracht, M. Neumann and G. Rawitscher, *Integral Equation Method for the Continuous Spectrum Radial Schrödinger Equation*, J. of Comput. Phys. **134**, 134-149 (1997);
 - [7] R. A. Gonzales, S.-Y. Kang, I. Koltracht and G. Rawitscher, *Integral Equation Method for Coupled Schrödinger Equations*, J. of Comput. Phys. **153**, 160-202 (1999);
 - [8] L. Greengard and V. Rokhlin, *Commun. Pure Appl. Math.* **2**, 197 (1960).
 - [9] G. Rawitscher and I. Koltracht, *A spectral integral method for the solution of the Faddeev equations in configuration space*, Nucl. Phys. **A 737CF**, S314-S316 (2004);

- [10] B. Mihaila and I. Mihaila, *Numerical approximations using Chebyshev polynomial expansions: El-gendi's method revisited*, J. Phys. A: Math. Gen. **35**, 731-746 (2002), B. Mihaila and R.E. Shaw, *Parallel algorithm with spectral convergence for nonlinear integro-differential equations*, J. Phys. A: Math. Gen. **35**, 5315 (2002);
- [11] Gottlieb D and Orszag S A *Numerical analysis of Spectral Methods: Theory and Applications*", CBMS-NSF Regional Conference Series in Applied Mathematics #26, Society for Industrial and Applied Mathematics, Philadelphia PA 1977;
- [12] M. Abramowitz and I. Stegun (Eds.), *Handbook of Mathematical Functions* (Dover, New York, 1972)
- [13] C.W. Clenshaw and A. R. Curtis, *A method for numerical integration on an automatic computer*, Numer. Math. **2**, 197(1991);
- [14] I. S. Gradshteyn and I. M. Ryzhik, *Tables of Integrals, Series and Products*, (Academic Press, New York, 1980), Eqs. 7.355, p. 836.
- [15] G. H. Rawitscher, B. D. Esry, E. Tiesinga, J. P. Burke, Jr., and I Koltracht, *Comparison of numerical methods for the calculation of cold atom collisions*, J of Chem. Phys. **111**, 10418-10426 (1999).
- [16] The authors are grateful to Dr. Ionel Simbotin for stimulating conversations regarding this method involving two rather than three contiguous partitions..
- [17] R. L. Burden and J. Douglas Faires, *Numerical Analysis*, 7th ed., Brooks/Cole (2001);
- [18] Ed. R. Smith and R. J. Henry, *Noniterative Integral-Equation Approach to Scattering Problems*, Phys. Rev. **A 7**, 1585-1590 (1973) and references therein; R. J. W. Henry, S. P. Rountree and Ed R. Smith, *A general program to calculate atomic continuum processes using the NIEM method*, Comp. Phys. Comm., **23**, 233-273 (1981);
- [19] G. H. Rawitscher, S. -Y. Kang, I. Koltracht, *A novel method for the solution of the Schrödinger equation in the presence of exchange terms*, J. Chem. Phys. **118**, 9149-9156 (2003);
- [20] W. N. Sams and D. J. Kouri, *Noniterative Solutions of Integral Equations for Scattering. I. Single Channels*, J. Chem. Phys. **51**, 4809-4814 (1969).
- [21] I. Bray, *Calculation of electron impact total, ionization, and nonbreakup cross sections from the 3S and 3P states of sodium*, Phys. Rev. Lett. **73**, 1088-1090 (1994); M. A. Haynes, B. Lohmann, I. Bray, K. Bartschat, *Ionization of rubidium by 50-eV electrons*, Phys. Rev. A, At. Mol. Opt. Phys. (USA) **69**, 44704-1-4 (2004); C. W. McCurdy, D. A. Horner, T. N.

- Rescigno, F. Martin, *Theoretical treatment of double photoionization of helium using a B-spline implementation of exterior complex scaling*, Phys. Rev. **A 69**, 32707-1-12 (2004);
- [22] H. R. Thorsheim, J. Weiner and P. S. Julienne, *Laser-induced photoassociation of ultracold sodium atoms*, Phys. Rev. Lett., **58**, 2420-2423 (1987); A. N. Nikolov, E. E. Eyler, X. T. Wang, J. Li, H. Wang, W. C. Stwalley and P. L. Gould, , *Observation of ultracold ground-state potassium molecules*, Phys. Rev. Lett. **82**, 703-706, (1999); J. Leonard, A. P. Mosk, M. Walhout, P. van der Straten, M. Leduc, C. Cohen-Tannoudji, *Analysis of photoassociation spectra for giant helium dimers*, Phys. Rev. **A 69**, 32702-1-12 (2004);
- [23] S. Giorgini, L. P. Pitaevskii, and S. Stringari *Condensate fraction and critical temperature of a trapped interacting Bose gas*, Phys. Rev. **A 54**, R4633-R4636 (1996);
- [24] C. P. Search, W. Zhang, and P. Meystre, *Inhibiting Three-Body Recombination in Atomic Bose-Einstein Condensates*, Phys. Rev. Lett. **92**, 140401-1-4 (2004);
- [25] M. Aymar, Chris H. Greene, and E. Luc-Koenig, *Multichannel Rydberg spectroscopy of complex atoms*, Revs. Mod. Phys. **68**,1015-1123 (1996); J. Shertzer and J. Botero, *Finite-element analysis of electron-hydrogen scattering*, Phys. Rev. A **49**, 3673-3679 (1994).
- [26] R. G. Gordon, J. Chem. Phys. **51**, 14 (1969); *Methods in Computational Physics*, edited by B. J. Alder, S. Fernbach, and M. Rotenberg (Academic , New York, 1971), Vol 10, pp. 81-110; F. H. Mies, Phys. Rev. **A7**, 957 (1973).
- [27] J. M. Hutson, S. Green, MOLSCAT computer code, version 14 (1994), distributed by Collaborative Computational Project No 6, Engineering and Physical Sciences Research Council, UK.
- [28] The authors are thankful to Dr. Ionel Simbotin, at the Dept. of Physics, University of Connecticut, for having performed the calculation with the MOLSCAT code.
- [29] L. Gr. Ixaru, *LILIX-A package for the solution of the coupled channel Schrödinger equation*, Comput. Phys. Commun. **147**, 834-852 (2002);
- [30] J. J. Kolata, V. Guimaraes, D. Peterson, P. Santi, R. White-Stevens, P. A. DeYoung, G. F. Peaslee, B. Hughey, B. Atalla, M. Kern, P. L. Jolivet, J. A. Zimmerman, M. Y. Lee, F. D. Becchetti, E. F. Aguilera, E. Martinez-Quiroz, J. D. Hinnefeld, *Sub-barrier fusion of ^6He with ^{209}Bi* , Phys. Rev. Lett. **81**, 4580-4583 (1998);
- [31] F. Michel, F. Brau, G. Reidemeister, S. Ohkubo, S. *Barrier-wave-internal-wave interference and Airy minima in $^{16}\text{O}+^{16}\text{O}$ elastic scattering*, Phys. Rev. Lett. **85**, 1823-1826 (2000);

- [32] J. M. Alexander, M. T. Magda, S. Landowne, *Inverse reactions and the statistical evaporation model: ingoing-wave boundary-condition and optical models*, Phys. Rev. C **42**, 1092-1098 (1990);
- [33] E. Bodo, F. A. Gianturco, and A. Dalgarno, *F+D2 reaction at ultracold temperatures*, J. of Chem. Phys. **116**, 9222-9227 (2002);
- [34] A. P. M. Morse, Phys. Rev. **34**, 57 (1929).
- [35] G. Rawitscher, C. Merow, M. Nguyen, I. Simbotin; *Am. J. of Phys.* **70**, 935 (2002);
- [36] Calculation performed by Dr. E. Zerrad. at Delaware State University, Dover, DE.
- [37] The authors are thankful to Dr. N. Balakrishnan of the Institute for Theoretical and Molecular Physics, at the Harvard-Smithsonian Center for Astrophysics, Cambridge MA 02138, and Dr. Ionel Simbotin, at the Dept. of Physics, University of Connecticut, for having performed the calculation with the MOLSCAT code.
- [38] W. B. Gragg, *On Extrapolation Algorithms for Ordinary Initial Value Problems*, SIAM J, ser B, *Numer. Anal.***2**, 384-403 (1965);
- [39] J. A. Christley and I. J. Thompson, *CRCWFN: coupled real Coulomb wavefunctions*, Comput. Phys. Commun. **79**, 143-155 (1994). The authors are indebted to Professor Thompson for helpful comments, upon which this paragraph is based.
- [40] J. C. Light and R. B. Walker, *An R matrix approach to the solution of coupled equations for atom-molecule reactive scattering*, J. Chem. Phys. **65**, 4272-4282 (1976);
- [41] V. M. Burke and C. J. Noble, *Farm — A flexible asymptotic R-matrix package*, Comp. Phys. Comm. **85**, 471-500 (1995);
- [42] K. L. Baluja, P. J. Burke, and L. A. Morgan, *R-matrix propagation program for solving coupled second-order differential equations*, Comput. Phys. Commun. **27**, 299-307 (1982);
- [43] G. Rawitscher, *Positive energy Weinberg states for the solution of scattering problems*, Phys. Rev. C **25**, 2196-2213 (1982); G. H. Rawitscher and G. Delic, *Sturmian representation of the optical model potential due to coupling to inelastic channels*, Phys. Rev. C **29**, 1153-1162 (1984);
- [44] K. Amos, L. Canton, G. Pisent, J. P. Svenne, and D. van der Knijff, *An algebraic solution of the multichannel problem applied to low energy nucleon–nucleus scattering*, Nucl. Phys. **A728**, 65-69 (2003);
- [45] J. Stoer and R. Bulirsch, *Introduction to Numerical Analysis*, 2nd ed. (Springer Verlag, 1992),

section 7.3.5.5.